Received –; | Revised –; | Accepted –

DOI: xxx/xxxx

RESEARCH ARTICLE

# Local discontinuous Galerkin method for distributed-order time-fractional diffusion-wave equation: Application of Laplace transform

Hadi Mohammadi Firouzjaei | Hojatollah Adibi* | Mehdi Dehghan

Department of Applied Mathematics, Faculty of Mathematics and Computer Sciences, Amirkabir University of Technology, No. 424, Hafez Ave 15914, Tehran, Iran

**Correspondence**
*Hojatollah Adibi, Department of Applied Mathematics, Faculty of Mathematics and Computer Sciences, Amirkabir University of Technology, No. 424, Hafez Ave, 15914 Tehran, Iran. Email: adibih@aut.ac.ir

**Summary**

In this paper, the Laplace transform combined with the local discontinuous Galerkin method is used for distributed-order time-fractional diffusion-wave equation. In this method, at first, we convert the equation to some time-independent problems by Laplace transform. Then we can solve these stationary equations by the local discontinuous Galerkin method to discretize diffusion operators at the same time. Then, by using a numerical inversion of the Laplace transform we can find the solutions of the original equation. One of the advantages of this procedure is its parallel implementation. Another advantage of this approach is that the number of stationary problems that should be solved is much less than that are needed in time-marching methods. Finally, some numerical experiments have been provided to show the accuracy and efficiency of the method.

**KEYWORDS:**
Distributed-order time-fractional diffusion-wave equation, Local discontinuous Galerkin method, Laplace transform, Parallel algorithms.

## 1 | INTRODUCTION

Fractional differential equations are widely used to model anomalous behavior of a system. This application has brought a lot of interest to scientists and engineers [1,2,3]. The fractional diffusion equation (FDE) is one of the fractional PDEs which has been extremely popular, see e.g. [4,5]. Nowadays instead of the classical diffusion equations, FDEs have attracted broad concentration. Because the FDE is a generalization of a diffusion equation that can be used to describe an anomalous diffusion phenomenon [6]. A time-fractional diffusion equation is achieved by replacing the integer time derivative with a time-fractional derivative in a diffusion equation. FDEs can be employed in modeling some problems in mechanical systems, models of a variety of biological processes [7], control and robotics [8] and many other areas of applications. Some numerical methods based on the Laplace transform method are utilized for time-fractional diffusion and time-fractional diffusion-wave equations [9,10,11].

There are various researches [12,13] about Laplace transform to deal with time derivative. In this method, at first, we convert these equations to some time-independent problems by Laplace transform. We will solve these stationary equations by space discretization methods to discretize diffusion operators of each stationary equation. The solution is recovered by numerical inversion of the Laplace transform. The major difference between this method and the time-marching method is that in this approach fewer linear systems are solved. Moreover, there is no need to solve them in series and we can do it simultaneously. However, requiring the Laplace transform of the source term and not giving good accuracy around t=0 are the restrictions in

this method. Gavrilyuk and Makarov in [14] overcame these challenges by introducing a modification of this method. McLean and Thomée in [15,16] used this modification and analyzed that based on maximum and $L_2$ norms for fractional-order evolution equations. In [12,13] when the Laplace transform method used for time discretization, the finite element method (FEM) used for the discretization of space operators. The simplicity of the implementation of the radial basis function (RBF) method instead of the FEM caused that Laplace transform has been combined with the RBFs for the parabolic equations on the sphere [17,18]. The Laplace transform with the Fourier transform, used to the analytical study of the distributed-order time-fractional (DOTF) sub-diffusion [6] and DOTF diffusion-wave equations [19].

In this paper, we will consider the following time distributed-order diffusion model

$$\int_{\beta_1}^{\beta_2} \mathcal{W}(\beta) {}_0^C D_t^\beta u(\mathbf{x},t) d\beta = \Delta u(\mathbf{x},t) + f(\mathbf{x},t), \quad (\mathbf{x},t) \in \Omega \times (0,T], \tag{1}$$

in which $\mathcal{W}(\beta)$ is the weight function of the distribution of order $\beta$ [20]. The model is divided into three kinds of equations. Assuming $\beta_1 := inf\{\beta | \beta \in supp\ \mathcal{W}(\beta)\}$ and $\beta_2 := sup\{\beta | \beta \in supp\ \mathcal{W}(\beta)\}$. When $0 < \beta_1 \leq 1 < \beta_2 \leq 2$, Eq. (1) is a DOTF diffusion-wave equation, also when, $\beta_2 \leq 1$, Eq. (1) is a DOTF diffusion equation and if $\beta_1 > 1$, Eq. (1) is a DOTF wave equation [20]. Some researchers have proposed numerical methods to solve the distributed-order differential equations . The finite difference method [21,22,23,24], finite difference/spectral method [25,26,27], local discontinuous Galerkin (LDG) method [28] and some meshless methods [29,30,31] have been applied for the solution of distributed-order differential equations. In this study we provide a numerical method for solving two sub-classes of Eq. (1). We consider DOTF diffusion equation [32,33]

$$\begin{cases} \int_0^1 \mathcal{W}(\beta) {}_0^C D_t^\beta u(\mathbf{x},t) d\beta = \Delta u(\mathbf{x},t) + f(\mathbf{x},t), \quad (\mathbf{x},t) \in \Omega \times (0,T], \\ u(\mathbf{x},0) = \psi(\mathbf{x}), \quad \mathbf{x} \in \Omega, \\ u(\mathbf{x},t) = 0, \quad (\mathbf{x},t) \in \partial\Omega \times (0,T], \end{cases} \tag{2}$$

which is investigated and analyzed by Jin et al.. They used the Laplace transform based on the FEM to recover the numerical solution of Eq. (2) [33].

The DOTF diffusion-wave equation is as

$$\begin{cases} \int_{\beta_1}^{\beta_2} \mathcal{W}(\beta) {}_0^C D_t^\beta u(\mathbf{x},t) d\beta = \Delta u(\mathbf{x},t) + f(\mathbf{x},t), \quad (\mathbf{x},t) \in \Omega \times (0,T], \\ u(\mathbf{x},0) = \psi(\mathbf{x}), \quad \mathbf{x} \in \Omega, \\ \frac{\partial}{\partial t} u(\mathbf{x},0) = \varphi(\mathbf{x}), \quad (x,0) \in \Omega, \\ u(\mathbf{x},t) = 0, \quad (\mathbf{x},t) \in \partial\Omega \times (0,T], \end{cases} \tag{3}$$

where $\beta_1 > 0$ and $1 < \beta_2 \leq 2$. We stated that Eq. (3) describes DOTF wave equation for $\beta_1 > 1$ and $\beta_2 \leq 2$. In [21] authors proposed a compact difference scheme when $\beta_1 = 1$ and $\beta_2 = 2$.

Let us consider Eq. (2). When we have $\mathcal{W}(\beta) = \delta(\beta - \alpha)$ where $\delta(\cdot)$ is the Dirac Delta function, Eq. (2) reduces to

$$\begin{cases} {}_0^C D_t^\alpha u(\mathbf{x},t) = \Delta u(\mathbf{x},t) + f(\mathbf{x},t), \quad (\mathbf{x},t) \in \Omega \times (0,T], \\ u(\mathbf{x},0) = \psi(\mathbf{x}), \quad \mathbf{x} \in \Omega, \\ u(\mathbf{x},t) = 0, \quad (\mathbf{x},t) \in \partial\Omega \times (0,T], \end{cases} \tag{4}$$

where $0 < \alpha < 1$. When $\alpha \to 1$, Eq. (4) tends to parabolic (heat) equation. Laplace transform based on the FEM studied and analyzed for the parabolic equation in [12,13]. Eq. (4) is known as sub-diffusive PDE [9]. The Laplace transform coupled with the Chebyshev spectral collocation method is applied to recover solution of Eq. (4) in one-dimensional case. [9]. Uddin et al. [10] worked on Eq. (4) with use of the local meshless method.

Considering Eq. (3), again when $\mathcal{W}(\beta) = \delta(\beta - \alpha)$ Eq. (3) reduces to

$$\begin{cases} {}_0^C D_t^\alpha u(\mathbf{x},t) = \Delta u(\mathbf{x},t) + f(\mathbf{x},t), \quad (\mathbf{x},t) \in \Omega \times (0,T], \\ u(\mathbf{x},0) = \psi(\mathbf{x}), \quad \mathbf{x} \in \Omega, \\ \frac{\partial}{\partial t} u(\mathbf{x},0) = \varphi(\mathbf{x}), \quad (x,0) \in \Omega, \\ u(\mathbf{x},t) = 0, \quad (\mathbf{x},t) \in \partial\Omega \times (0,T], \end{cases} \tag{5}$$

where $1 < \alpha < 2$. When $\alpha \to 2$, Eq. (5) tends to wave equation. The Laplace transform method combined with a localized meshless method and was applied in [11] for solving Eq. (5).

## 1.1 | Motivations

The main aim of the current work is to implement a numerical method for the solutions of equations (2) and (3). We use the Laplace transform method based on the LDG method. The Laplace transform and time-marching methods have different approaches for time discretization. The main restriction of the time-marching methods is Courant-Friedrichs-Lewy (CFL) condition and here we employ the Laplace transform method via the LDG scheme to avoid the time-stepping issue. This method not only can be applied parallelly but also maintains good accuracy. In Section 2 we will present a brief description of some ideas which is needed later. Section 3 is dedicated to the implementation of the Laplace transform method based on the LDG method. In Section 4 we present some numerical results for both equations (2) and (3). Section 5 includes the conclusion.

## 2 | PRELIMINARIES

**Definition 1.** Caputo fractional derivative which is introduced by Michele Caputo[34], is defined as

$$ {}_0^C D_t^\beta f(t) = \frac{1}{\Gamma(n-\beta)} \int_0^t \frac{f^{(n)}(z)}{(t-z)^{\beta+1-n}}\, dz, \quad n-1 < \beta \le n. \tag{6} $$

Here, when $0 < \beta \le 1$, for $n = 1$, Eq. (6) gives

$$ {}_0^C D_t^\beta f(t) = \frac{1}{\Gamma(1-\beta)} \int_0^t \frac{f'(z)}{(t-z)^{\beta}}\, dz, \quad 0 < \beta \le 1. $$

Also for $n = 2$ and $1 < \beta \le 2$ the definition is

$$ {}_0^C D_t^\beta f(t) = \frac{1}{\Gamma(2-\beta)} \int_0^t \frac{f''(z)}{(t-z)^{\beta-1}}\, dz, \quad 1 < \beta \le 2. $$

**Theorem 1.** [34] (Laplace transform formula for Caputo fractional derivative). Using definition 1, assuming $\beta > 0$, the Laplace transform formula for the Caputo fractional derivative is as follows:

$$ \mathcal{L}\{{}_0^C D_t^\beta f(t)\} = s^\beta F(s) - \sum_{k=0}^{n-1} s^{\beta-k-1} f^k(0), \quad n-1 < \beta \le n, \tag{7} $$

where $F(s)$ is the Laplace transform of $f(t)$.

**Corollary 1.** [34] When $n = 1$, $0 < \beta \le 1$, then Eq. (7) reduces to

$$ \mathcal{L}\{{}_0^C D_t^\beta f(t)\} = s^\beta F(s) - s^{\beta-1} f(0), \quad 0 < \beta \le 1, $$

and for $n = 2$, $1 < \beta \le 2$, Eq. (7) gives

$$ \mathcal{L}\{{}_0^C D_t^\beta f(t)\} = s^\beta F(s) - s^{\beta-1} f(0) - s^{\beta-2} f'(0), \quad 1 < \beta \le 2. $$

## 3 | TIME DISCRETIZATION

This section is devoted to the time discretization of Eqs. (2) and (3). Sheen et al.[12,13] presented Laplace transform approach to solve partial differential equations for discretizing temporal term. The Laplace transform approach for time discretization and continuous Galerkin finite element method is used[33] for space discretization to recover the solutions of DOTF diffusion equation. We follow the same approach that they have done but with some differences. Local discontinuous Galerkin is replaced by Galerkin finite element method. That is; at first we review the approach followed in[33], but LDG is used instead of Galerkin FEM to achieve higher order accuracy. After that we implement the Laplace transform based on LDG method for distributed-order time-fractional diffusion-wave equation. Also, the modified version of the method which is presented to find the solution of heat equation in[14] is applied for DOTF diffusion-wave equation.

**First case:** Eq. (2). Applying the Laplace transform and Corollary 1 to Eq. (2) gives[33]

$$\int_0^1 \mathcal{W}(\beta)\left(s^\beta \mathcal{U}(\mathbf{x},s) - s^{\beta-1}u_0\right)\, d\beta - \Delta\mathcal{U}(\mathbf{x},s) = \mathcal{F}(\mathbf{x},s),$$

and by simplifying it we obtain[33]

$$\left(\int_0^1 \mathcal{W}(\beta)s^\beta\, d\beta\, \mathcal{I} - \Delta\right)\mathcal{U}(\mathbf{x},s) = \int_0^1 \mathcal{W}(\beta)s^{\beta-1}\, d\beta\, u_0 + \mathcal{F}(\mathbf{x},s), \tag{8}$$

in which $\mathcal{I}$ denotes the identity operator and $\mathcal{W}(\beta)$ is a known function. Define $m_1(s) = \int_0^1 \mathcal{W}(\beta)s^\beta d\beta$ and $m_2(s) = \int_0^1 \mathcal{W}(\beta)s^{\beta-1}d\beta$, which can be evaluated exactly or numerically. By substituting $m_1(s)$ and $m_2(s)$ in Eq. (8) we rewrite Eq. (8) as[33]

$$\left(m_1(s)\mathcal{I} - \Delta\right)\mathcal{U}(\mathbf{x},s) = m_2(s)u_0 + \mathcal{F}(\mathbf{x},s), \tag{9}$$

which can be rewritten as

$$\mathcal{U}(\mathbf{x},s) = \widehat{\varepsilon_1(s)}g_1(s), \tag{10}$$

where $\widehat{\varepsilon_1(s)} = \left(m_1(s)\mathcal{I} - \Delta\right)^{-1}$ and $g_1(s) = m_2(s)u_0 + \mathcal{F}(\mathbf{x},s)$. We recover the solution by the inversion Laplace

$$u(t) = \mathcal{L}^{-1}\left\{\mathcal{U}(\mathbf{x},s)\right\} = \frac{1}{2\pi i}\int_\Gamma e^{st}\mathcal{U}(\mathbf{x},s)\, ds, \quad \text{for } t > 0, \tag{11}$$

where the path of integration, $\Gamma$, is the line $Real(s) = \sigma$, with $\sigma \geq \sigma_0 > 0$ and with an increasing imaginary part, i.e.

$$u(t) = \mathcal{L}^{-1}\left\{\mathcal{U}(\mathbf{x},s)\right\} = \frac{1}{2\pi i}\int_{\sigma-i\infty}^{\sigma+i\infty} e^{st}\mathcal{U}(\mathbf{x},s)\, ds, \quad \text{for } t > 0,\ \ \sigma > \sigma_0.$$

The above integral is known as Bromwich integral[9]. When a contour of integration as $s = s(\zeta)$ is considered we obtain

$$u(t) = \mathcal{L}^{-1}\left\{\mathcal{U}(\mathbf{x},s)\right\} = \frac{1}{2\pi i}\int_{-\infty}^{\infty} e^{s(\zeta)t}\mathcal{U}(\mathbf{x},s(\zeta))s'(\zeta)\, d\zeta, \tag{12}$$

and this integral is calculated numerically via well-known quadrature rules like trapezoidal rule with step size $k$ as

$$u_{N_{Lap}}(t) = \frac{k}{2\pi i}\sum_{j=-N_{Lap}}^{N_{Lap}} e^{s_j t}\mathcal{U}(\mathbf{x},s_j)s_j',$$

in which $s_j = s(\zeta_j)$, $s_j' = s'(\zeta_j)$, $\zeta_j = jk$ and

$$\mathcal{U}(\mathbf{x},s_j) = \widehat{\varepsilon_1(s_j)}g_1(s_j), \quad -N_{Lap} \leq j \leq N_{Lap}. \tag{13}$$

In all procedures following in this paper, we choose a contour integration like

$$s(\zeta) = \mu(i\zeta + 1)^2, \quad -\infty < \zeta < \infty,$$

or

$$s(\zeta) = \mu(1 + sin(i\zeta - c)), \quad -\infty < \zeta < \infty,$$

where the parameters are optimized in[9].

**Second case:** Eq. (3). Taking Laplace transform from Eq. (3) and applying Corollary 1 gives

$$\int_{\beta_1}^{\beta_2} \mathcal{W}(\beta)\left((s^\beta \mathcal{U}(\mathbf{x},s) - s^{\beta-1}u_0 - s^{\beta-2}u_0'\right)\, d\beta - \Delta\mathcal{U}(\mathbf{x},s) = \mathcal{F}(\mathbf{x},s),$$

and subsequently

$$\left(\int_{\beta_1}^{\beta_2} \mathcal{W}(\beta)s^{\beta}d\beta \;\; \mathcal{I}-\Delta\right)\mathcal{U}(\mathbf{x},s)=\int_{\beta_1}^{\beta_2}\mathcal{W}(\beta)s^{\beta-1}d\beta u_0+\int_{\beta_1}^{\beta_2}\mathcal{W}(\beta)s^{\beta-2}d\beta u_0^{'}+\mathcal{F}(\mathbf{x},s),$$

in which $\mathcal{W}(\beta)$ is a known function, so we denote

$$m_1^{'}(s)=\int_{\beta_1}^{\beta_2}\mathcal{W}(\beta)s^{\beta}d\beta,\; m_2^{'}(s)=\int_{\beta_1}^{\beta_2}\mathcal{W}(\beta)s^{\beta-1}d\beta,\; m_3^{'}(s)=\int_{\beta_1}^{\beta_2}\mathcal{W}(\beta)s^{\beta-2}d\beta.$$

Note that $m'_i(s)$ can be evaluated exactly or numerically for $i=1,2,3$. Then Eq. (12) can be simplified to

$$\left(m_1^{'}(s)\mathcal{I}-\Delta\right)\mathcal{U}(\mathbf{x},s)=m_2^{'}(s)u_0+m_3^{'}(s)u_0^{'}+\mathcal{F}(\mathbf{x},s),$$

or briefly

$$\mathcal{U}(\mathbf{x},s)=\widehat{\varepsilon_2(s)}g_2(s),$$

where

$$\widehat{\varepsilon_2(s)}=\left(m_1^{'}(s)\mathcal{I}-\Delta\right)^{-1},\quad g_2(s)=m_2^{'}(s)u_0+m_3^{'}(s)u_0^{'}+\mathcal{F}(\mathbf{x},s).$$

By exactly the same procedure as in the first case the solution is recovered by using the inversion Laplace transform and the associated integral is calculated via

$$\tilde{u}_{N_{lap}}(t)=\frac{k}{2\pi i}\sum_{j=-N_{lap}}^{N_{lap}}e^{s_jt}\mathcal{U}(\mathbf{x},s_j)s_j^{'},$$

in which $s_j=s(\zeta_j)$, $s_j^{'}=s^{'}(\zeta_j)$, $\zeta_j=jk$ and

$$\mathcal{U}(\mathbf{x},s_j)=\widehat{\varepsilon_2(s_j)}g_2(s_j),\quad -N_{lap}\le j\le N_{lap}. \tag{14}$$

**Remark 1.** The finite element method is a well-known technique for space discretization. But in this article local discontinuous Galerkin method is used for spatial discretization to obtain a technique with high order accuracy. Here the discretization operator that we will use is the one which has been introduced in [35].

**Remark 2.** In mentioned method, the Laplace transform method combined with the LDG method, Eqs. (13) and (14) have to be solved for each $s_j$, $-N_{lap}\le j\le N_{lap}$. Also, all of these equations can be solved simultaneously. This is the main advantage of this method which is called parallel method [12,13]. The reason of such naming is that these problems are completely independent. Therefore, these equations can be solved on separate processors. In contrast, the time-marching methods are not able to be solved parallelly [12].

**Remark 3.** It is notable that in this procedure we need to evaluate the Laplace transform of the source term $f(x,t)$ which might be difficult. The authors of [14] have modified this method in which the Laplace transform of the source term $f(x,t)$ is no longer needed. It is also used for fractional-order equations [15,16].

We review this modification [14,15,16] for first case. It's straightforward for the second case. Putting $f\equiv 0$ in Eq. (9) gives

$$\left(m_1(s)\mathcal{I}-\Delta\right)\mathcal{U}(\mathbf{x},s)=m_2(s)u_0.$$

Therefore the solution of Eq. (9) is as follows

$$u(t)=\varepsilon_1(t)\left(m_2(s)u_0\right),$$

where we define the operator $\varepsilon_1(t)$ for an arbitrary function $Q$ as

$$\varepsilon_1(t)\left(Q\right)=\frac{1}{2\pi i}\int_{\Gamma}e^{st}\left(m_1(s)\mathcal{I}-\Delta\right)^{-1}\left(Q\right)\,ds. \tag{15}$$

Now getting back to the inhomogeneous case, the solution can be obtained by (11) and Duhamel formula [14,16]

$$u(t) = \varepsilon_1(t)\left(m_2(s)u_0\right) + \frac{1}{2\pi i}\int_{\Gamma} e^{st}\widehat{\varepsilon_1(s)}\mathcal{F}(\mathbf{x}, s)\,ds \tag{16}$$

$$= \varepsilon_1(t)\left(m_2(s)u_0\right) + \int_0^t \varepsilon_1(t-\tau)f(\mathbf{x}, \tau)\,d\tau.$$

Putting Eq. (15) in (16) gives

$$u(t) = \frac{1}{2\pi i}\int_{\Gamma}\left(m_1(s)\mathcal{I} - \Delta\right)^{-1}\left(e^{st}m_2(s)u_0 + \int_0^t e^{s(t-\tau)}f(\mathbf{x}, \tau)\,d\tau\right)ds,$$

in which the path of integration, $\Gamma$, is the line $Real(s) = \sigma$, with $\sigma \geq \sigma_0 > 0$ and with an increasing imaginary part, i.e.

$$u(t) = \frac{1}{2\pi i}\int_{\sigma-i\infty}^{\sigma+i\infty}\widetilde{\mathcal{V}(\mathbf{x}, s)}\,ds, \text{ for } t > 0, \quad \sigma > \sigma_0, \tag{17}$$

where

$$\widetilde{\mathcal{V}(\mathbf{x}, s)} = \left(m_1(s)\mathcal{I} - \Delta\right)^{-1}\left(e^{st}m_2(s)u_0 + \int_0^t e^{s(t-\tau)}f(\mathbf{x}, \tau)\,d\tau\right).$$

As mentioned before, Eq. (17) is Bromwich integral. By considering a contour of integration as $s = s(\zeta)$ we have

$$u(t) = \frac{1}{2\pi i}\int_{-\infty}^{\infty}\widetilde{\mathcal{V}(\mathbf{x}, s(\zeta))}s'(\zeta)\,d\zeta, \tag{18}$$

in which

$$\widetilde{\mathcal{V}(\mathbf{x}, s(\zeta))} = \left(m_1(s(\zeta))\mathcal{I} - \Delta\right)^{-1}\left(e^{s(\zeta)t}m_2(s(\zeta))u_0 + \int_0^t e^{s(\zeta)(t-\tau)}f(\mathbf{x}, \tau)\,d\tau\right).$$

The integral (18) can be calculated numerically. By exactly the same method just used for Eq. (12), the numerical solution of (2) can be evaluated as

$$\tilde{u}_{N_{lap}}(t) = \frac{k}{2\pi i}\sum_{j=-N_{lap}}^{N_{lap}}\widetilde{\mathcal{V}(\mathbf{x}, s_j)}s_j',$$

which $s_j = s(\zeta_j)$, $s_j' = s'(\zeta_j)$, $\zeta_j = jk$ and

$$\widetilde{\mathcal{V}(\mathbf{x}, s_j)} = \left(m_1(s_j)\mathcal{I} - \Delta\right)^{-1}\left(e^{s_j t}m_2(s_j)u_0 + \int_0^t e^{s_j(t-\tau)}f(\mathbf{x}, \tau)\,d\tau\right), \quad -N_{Lap} \leq j \leq N_{Lap}. \tag{19}$$

For the numerical integration (18), (19) have to be solved for each $s_j$, $-N_{lap} \leq j \leq N_{lap}$. Now the LDG method can used to discretize space. Notice that we can solve all of these equations simultaneously to take advantage of this method as mentioned in Remark. 2.

## 4 | RESULTS AND DISCUSSION

In this section, we present some examples to show the accuracy of the modified method. For each case, two examples are provided. The order of accuracy and maximum and $L_2$ errors of method are reported. More properly, the error norms are defined as

$$L_\infty = \max_{1\leq i\leq M}|\tilde{u}_i - u(x_i, T)|, \qquad L_2^2 = \int_\Omega (\tilde{u} - u)^2\,dx,$$

in which $T$ is final time and $\tilde{u}$ and $u$ are approximated and exact solutions of the equation, respectively.

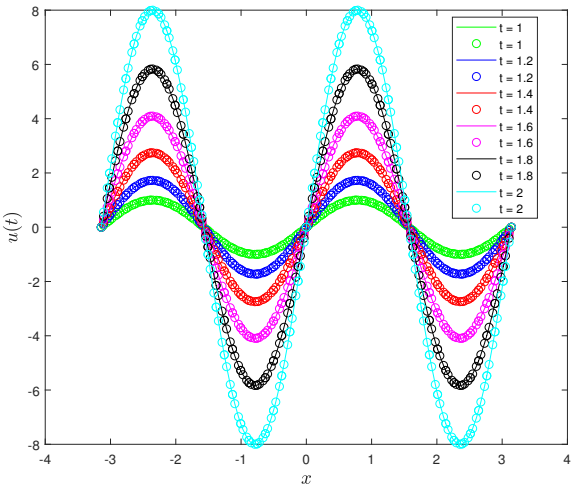


**FIGURE 1** Numerical results (solid line) and exact solution (circular marks) of Example 1 for various final times.

## 4.1 | Examples for the DOTF diffusion equation

**Example 1.** Here we present the numerical results of proposed method for time discretization of one-dimensional DOTF diffusion Eq. (2) as follows

$$\begin{cases} \int_0^1 \mathcal{W}(\beta)\, {}_0^C D_t^\beta u(x,t) d\beta = \Delta u(x,t) + f(x,t), \quad (x,t) \in \Omega \times (0,T], \\ u(x,0) = \psi(x), \quad x \in \Omega, \\ u(x,t) = 0, \quad (x,t) \in \partial\Omega \times (0,T]. \end{cases} \tag{20}$$

Consider the exact solution $u(x,t) = t^3 sin(2x)$ with $x \in [-\pi, \pi]$ and $\mathcal{W}(\beta) = \Gamma(4-\beta)$. The numerical and exact solutions of Eq. (2) are shown in Figure 1 for different final times. Also the errors in maximum norm are presented in Table 1 .

**Example 2.** For 2D example, two-dimensional DOTF diffusion equation is determined as

$$\begin{cases} \int_0^1 \mathcal{W}(\beta)\, {}_0^C D_t^\beta u(\mathbf{x},t) d\beta = \Delta u(\mathbf{x},t) + f, \quad \mathbf{x} = (x,y) \in \Omega;\ t \in (0,T], \\ u(\mathbf{x},0) = \psi(\mathbf{x}), \quad \mathbf{x} \in \Omega, \\ u(\mathbf{x},t) = 0, \quad (\mathbf{x},t) \in \partial\Omega \times (0,T]. \end{cases} \tag{21}$$

The exact solution $u(x,y,t) = t^3 sin(\pi x) sin(\pi y)$ with $\Omega = [-1,1] \times [-1,1]$ is considered for Eq. (2) with $\mathcal{W}(\beta) = \Gamma(4-\beta)$. The numerical results are shown in Figure 2 .

## 4.2 | Examples for the DOTF diffusion-wave equation

**Example 3.** Suppose the following equation

$$\begin{cases} \int_{\beta_1}^{\beta_2} \mathcal{W}(\beta)\, {}_0^C D_t^\beta u(x,t) d\beta = \Delta u(x,t) + f(x,t), \quad (x,t) \in \Omega \times (0,1], \\ u(x,0) = \psi(x), \quad x \in \Omega, \\ \frac{\partial}{\partial t} u(x,0) = \varphi(x), \quad (x,0) \in \Omega, \\ u(x,t) = 0, \quad (x,t) \in \partial\Omega \times (0,1], \end{cases} \tag{22}$$

has the exact solution $u(x;t) = t^4 sin(\frac{\pi}{2}x)$ with $x \in [-2,2]$ and $\mathcal{W}(\beta) = \Gamma(5-\beta)$. In this one-dimensional DOTF diffusion-wave equation $\beta_1 = 1$ and $\beta_2 = 2$. To depict the numerical and exact solutions of Eq. (22) we refer reader to Figure 3 . Also the errors in maximum norm obtained by Laplace transform and the quadrature rule used are presented in Table 2 .

**TABLE 1** $L_2$- and maximum-norm of errors obtained for Example 1

| | $N_{lap} = 10$ | | $N_{lap} = 20$ | | $N_{lap} = 40$ | | $N_{lap} = 80$ | |
|---|---|---|---|---|---|---|---|---|
| | $L_\infty$ | $L_2$ | $L_\infty$ | $L_2$ | $L_\infty$ | $L_2$ | $L_\infty$ | $L_2$ |
| $p = 1$ | | | | | | | | |
| $N_{DG}$ | | | | | | | | |
| 10 | 1.1762e-01 | 1.2648e-01 | 1.0869e-01 | 1.1258e-01 | 1.0783e-01 | 1.1140e-01 | 1.0781e-01 | 1.1137e-01 |
| 20 | 5.2180e-02 | 6.1183e-02 | 4.3303e-02 | 4.5861e-02 | 4.2444e-02 | 4.4886e-02 | 4.2419e-02 | 4.4860e-02 |
| 40 | 2.5874e-02 | 3.7155e-02 | 1.6505e-02 | 1.7523e-02 | 1.6054e-02 | 1.6641e-02 | 1.6040e-02 | 1.6621e-02 |
| 80 | 1.8257e-02 | 3.0898e-02 | 5.8378e-03 | 6.6727e-03 | 5.3851e-03 | 5.5799e-03 | 5.3784e-03 | 5.5628e-03 |
| 160 | 1.6805e-02 | 2.9609e-02 | 2.3627e-03 | 3.4146e-03 | 1.6338e-03 | 1.6982e-03 | 1.6271e-03 | 1.6819e-03 |
| 320 | 1.6563e-02 | 2.9337e-02 | 1.6220e-03 | 2.7889e-03 | 4.6208e-04 | 4.8982e-04 | 4.5509e-04 | 4.7032e-04 |
| 640 | 1.6517e-02 | 2.9274e-02 | 1.5220e-03 | 2.6906e-03 | 1.3284e-04 | 1.5774e-04 | 1.2102e-04 | 1.2517e-04 |
| $p = 2$ | | | | | | | | |
| $N_{DG}$ | | | | | | | | |
| 10 | 2.6332e-02 | 3.3542e-02 | 1.8314e-02 | 1.6703e-02 | 1.8313e-02 | 1.6488e-02 | 1.8313e-02 | 1.6488e-02 |
| 20 | 1.6493e-02 | 2.9323e-02 | 2.6727e-03 | 3.3760e-03 | 2.0881e-03 | 2.0695e-03 | 2.0881e-03 | 2.0680e-03 |
| 40 | 1.6514e-02 | 2.9254e-02 | 1.5198e-03 | 2.6791e-03 | 2.6107e-04 | 2.7210e-04 | 2.5705e-04 | 2.6091e-04 |
| 80 | 1.6505e-02 | 2.9253e-02 | 1.5049e-03 | 2.6665e-03 | 5.4608e-05 | 8.3834e-05 | 3.2131e-05 | 3.2843e-05 |
| 160 | 1.6504e-02 | 2.9253e-02 | 1.5043e-03 | 2.6663e-03 | 4.3743e-05 | 7.7251e-05 | 4.1066e-06 | 4.3476e-06 |
| 320 | 1.6504e-02 | 2.9253e-02 | 1.5043e-03 | 2.6663e-03 | 4.3525e-05 | 7.7143e-05 | 9.3894e-07 | 1.4922e-06 |
| 640 | 1.6504e-02 | 2.9253e-02 | 1.5043e-03 | 2.6663e-03 | 4.3522e-05 | 7.7141e-05 | 7.9270e-07 | 1.4018e-06 |

**TABLE 2** $L_2$- and maximum-norm of errors obtained for Example 3

| | $N_{lap} = 10$ | | $N_{lap} = 20$ | | $N_{lap} = 40$ | | $N_{lap} = 80$ | |
|---|---|---|---|---|---|---|---|---|
| | $L_\infty$ | $L_2$ | $L_\infty$ | $L_2$ | $L_\infty$ | $L_2$ | $L_\infty$ | $L_2$ |
| $p = 1$ | | | | | | | | |
| $N_{DG}$ | | | | | | | | |
| 10 | 3.0091e-02 | 2.5648e-02 | 2.9089e-02 | 2.4566e-02 | 2.8452e-02 | 2.4148e-02 | 1.6060e-02 | 1.3737e-02 |
| 20 | 1.2535e-02 | 1.0606e-02 | 1.8434e-02 | 1.5199e-02 | 1.3078e-02 | 1.0789e-02 | 1.5649e-02 | 1.2899e-02 |
| 40 | 5.5633e-03 | 5.4820e-03 | 4.9121e-03 | 4.2011e-03 | 5.3055e-03 | 4.3442e-03 | 5.0735e-03 | 4.1540e-03 |
| 80 | 3.1145e-03 | 4.0171e-03 | 1.7565e-03 | 1.8825e-03 | 1.4333e-03 | 1.1720e-03 | 1.4288e-03 | 1.1673e-03 |
| 160 | 2.7279e-03 | 3.8265e-03 | 1.1187e-03 | 1.5272e-03 | 3.8314e-04 | 3.1807e-04 | 3.7902e-04 | 3.0952e-04 |
| 320 | 2.6956e-03 | 3.8095e-03 | 1.0666e-03 | 1.5051e-03 | 1.0863e-04 | 1.0369e-04 | 9.7724e-05 | 7.9800e-05 |
| 640 | 2.6923e-03 | 3.8073e-03 | 1.0643e-03 | 1.5050e-03 | 5.1875e-05 | 6.7423e-05 | 2.4819e-05 | 2.0264e-05 |
| $p = 2$ | | | | | | | | |
| $N_{DG}$ | | | | | | | | |
| 10 | 3.3924e-03 | 4.1600e-03 | 2.2539e-03 | 2.2566e-03 | 2.1254e-03 | 1.6821e-03 | 2.1255e-03 | 1.6808e-03 |
| 20 | 2.7018e-03 | 3.8124e-03 | 1.0826e-03 | 1.5198e-03 | 2.6197e-04 | 2.1813e-04 | 2.5760e-04 | 2.0863e-04 |
| 40 | 2.6924e-03 | 3.8068e-03 | 1.0639e-03 | 1.5057e-03 | 5.5796e-05 | 6.8823e-05 | 3.2112e-05 | 2.6174e-05 |
| 80 | 2.6918e-03 | 3.8068e-03 | 1.0645e-03 | 1.5055e-03 | 4.5227e-05 | 6.3740e-05 | 4.0427e-06 | 3.3482e-06 |
| 160 | 2.6918e-03 | 3.8068e-03 | 1.0645e-03 | 1.5055e-03 | 4.5013e-05 | 6.3656e-05 | 6.8675e-07 | 7.8089e-07 |
| 320 | 2.6918e-03 | 3.8068e-03 | 1.0645e-03 | 1.5055e-03 | 4.5011e-05 | 6.3655e-05 | 4.7352e-07 | 6.6592e-07 |
| 640 | 2.6918e-03 | 3.8066e-03 | 1.0645e-03 | 1.5055e-03 | 4.5011e-05 | 6.3655e-05 | 4.6952e-07 | 6.6396e-07 |

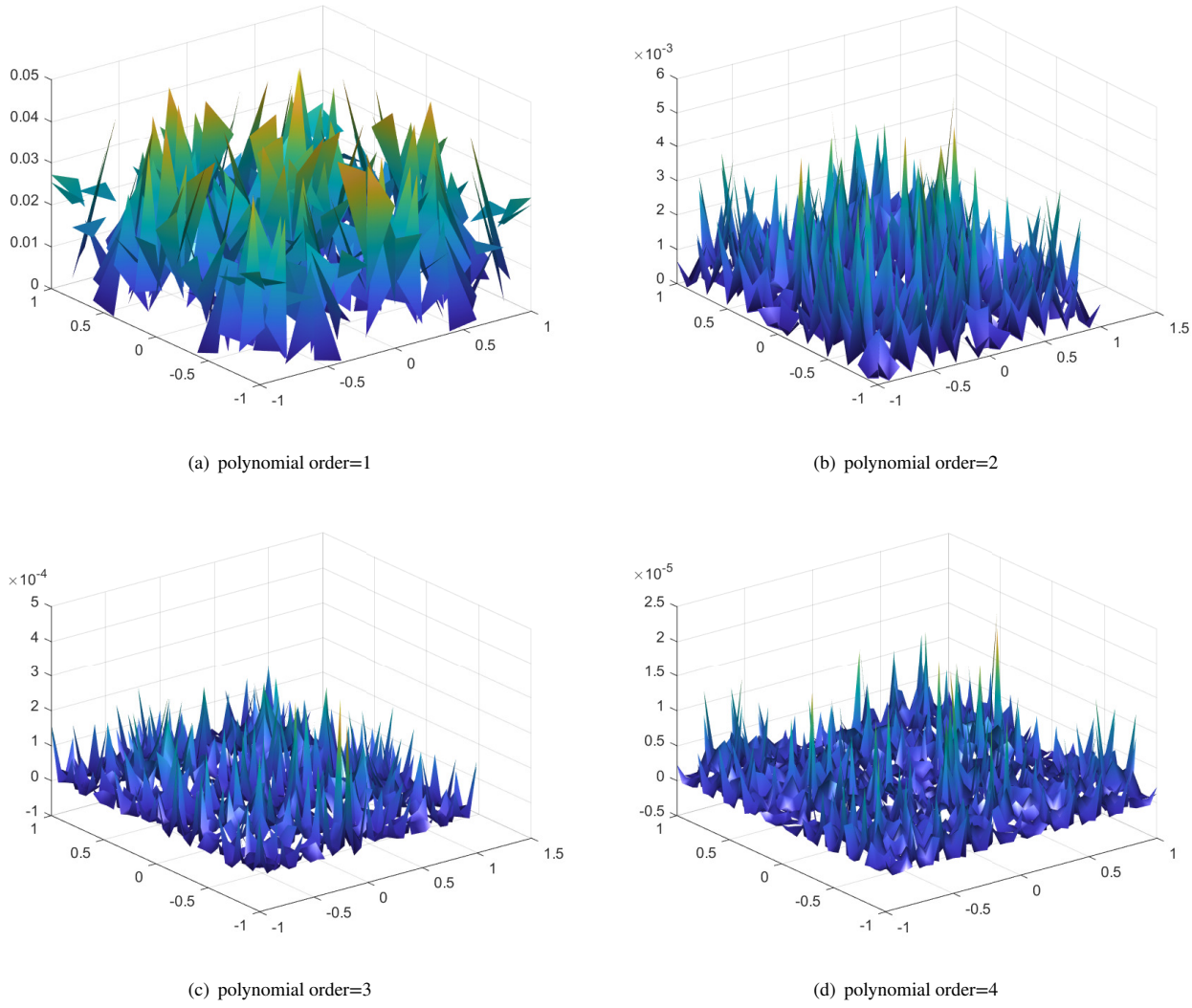

(a) polynomial order=1

(b) polynomial order=2

(c) polynomial order=3

(d) polynomial order=4

**FIGURE 2** Errors in maximum norm obtained for Example 2.

**Example 4.** Here the numerical results of two-dimensional DOTF diffusion-wave equation are presented. The exact solution is $u(x, y, t) = t^4 sin(\pi x) sin(\pi y)$ with $\Omega = [-1, 1] \times [-1, 1]$. In Eq. (3), $\mathcal{W}(\beta) = \Gamma(5 - \beta)$ is considered. The numerical and exact solutions of the Eq. (3) are shown in Figure 4 .

The results are shown in Tables 1 and 2 for some number of quadrature points, $N_{Lap}$, number of space elements, $N_{LDG}$ and the degree of polynomials, $p$, that were applied. In Figures 5 and 6 , it can be observed that when $h$ is the size of space elements, increasing $N_{Lap}$ leads to get convergence rate $O(h^{p+1})$. i.e. the results demonstrate that the proposed method suggested that the order of accuracy is $p + 1$ in both the $L_2$ and $L_\infty$ norms as we expected. Also, the errors of 2D examples are depicted in Figures 2 and 4 with several polynomial orders.

## 5 | CONCLUSION

In this paper we used the Laplace transform along with quadrature approach and obtained a parallel algorithm for distributed-order fractional differential equations. We utilized the local discontinuous Galerkin method for the discretization of space and Laplace transform which employed a quadrature formula for time discretization. To recover the solutions of time-dependent problems, we transformed equations to some time-independent problems by Laplace transform. The concluded stationary equations

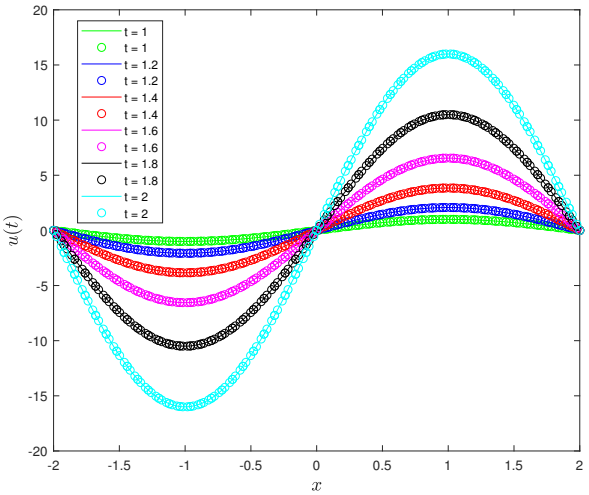


**FIGURE 3** Numerical results (solid line) and exact solution (circular marks) of Example 3 for various final times.

can be solved by the LDG method to discretize diffusion operators at the same time. By using a numerical inversion of the Laplace transform our solutions were recovered. The application of this method was to abandon the Courant-Friedrichs-Lewy (CFL) condition for solving time-dependent PDEs. Also, the Laplace transform combined with FEM used extensively but we substituted LDG instead of FEM to achieve a technique with high order accuracy. In fact, we used a modification of the method. The accuracy of the modified method was confirmed by presenting some examples.

## References

1. Deng W. Finite element method for the space and time fractional Fokker–Planck equation. *SIAM Journal on Numerical Analysis.* 2008;47(1):204–226.

2. Dehghan M, Manafian J, Saadatmandi A. The solution of the linear fractional partial differential equations using the homotopy analysis method. *Zeitschrift für Naturforschung-A.* 2010;65(11):935–949.

3. Dehghan M, Manafian J, Saadatmandi A. Solving nonlinear fractional partial differential equations using the homotopy analysis method. *Numerical Methods for Partial Differential Equations.* 2010;26(2):448–479.

4. Deng W, Hesthaven J S. Local discontinuous Galerkin methods for fractional diffusion equations. *ESAIM: Mathematical Modelling and Numerical Analysis.* 2013;47(6):1845–1864.

5. Qiu L, Deng W, Hesthaven J S. Nodal discontinuous Galerkin methods for fractional diffusion equations on 2D domain with triangular meshes. *Journal of Computational Physics.* 2015;298:678–694.

6. Naber M. Distributed order fractional sub-diffusion. *Fractals.* 2004;12(01):23–32.

7. Magin R L, Ingo C, Colon-Perez L, Triplett W, Mareci T H. Characterization of anomalous diffusion in porous biological tissues using fractional order derivatives and entropy. *Microporous and Mesoporous Materials.* 2013;178:39–43.

8. Cao Y, Ren W. Distributed formation control for fractional-order systems: dynamic interaction and absolute/relative damping. *Systems & Control Letters.* 2010;59(3-4):233–240.

9. Weideman J, Trefethen L. Parabolic and hyperbolic contours for computing the Bromwich integral. *Mathematics of Computation.* 2007;76(259):1341–1356.

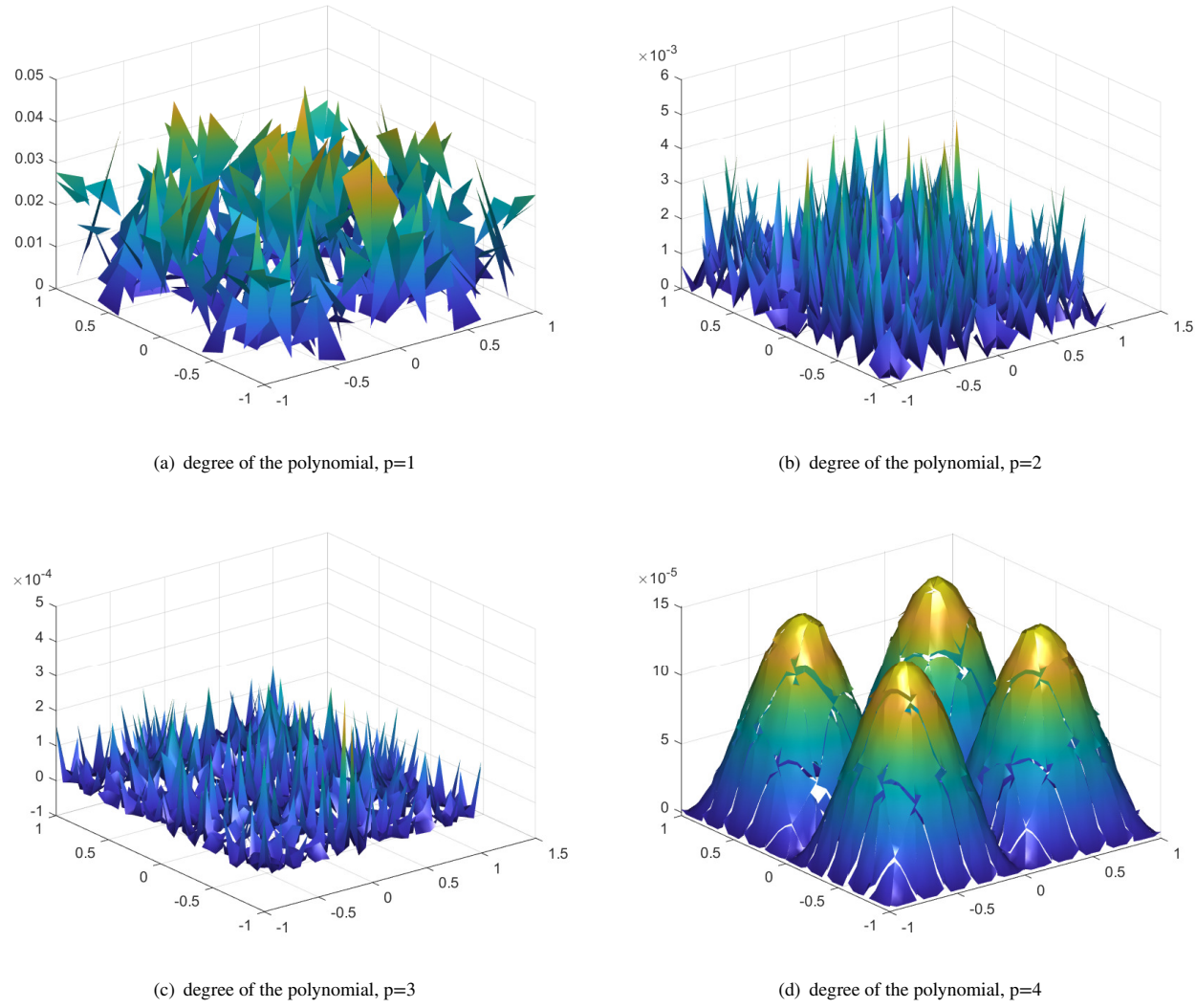


(a) degree of the polynomial, p=1

(b) degree of the polynomial, p=2

(c) degree of the polynomial, p=3

(d) degree of the polynomial, p=4

**FIGURE 4** Errors in maximum norm obtained for Example 4.

10. Uddin M, Kamran K, Usman M, Ali A. On the Laplace-transformed-based local meshless method for fractional-order diffusion equation. *International Journal for Computational Methods in Engineering Science and Mechanics.* 2018;19(3):221–225.

11. Uddin M, Kamran K, Ali A. A localized transform-based meshless method for solving time fractional wave-diffusion equation. *Engineering Analysis with Boundary Elements.* 2018;92:108–113.

12. Sheen D, Sloan I H, Thomée V. A parallel method for time-discretization of parabolic problems based on contour integral representation and quadrature. *Mathematics of Computation.* 2000;69(229):177–195.

13. Sheen D, Sloan I H, Thomée V. A parallel method for time discretization of parabolic equations based on Laplace transformation and quadrature. *IMA Journal of Numerical Analysis.* 2003;23(2):269–299.

14. Gavrilyuk I P, Makarov V L. Exponentially convergent algorithms for the operator exponential with applications to inhomogeneous problems in Banach spaces. *SIAM Journal on Numerical Analysis.* 2005;43(5):2144–2171.

15. McLean W, Thomée V. Maximum-norm error analysis of a numerical solution via Laplace transformation and quadrature of a fractional-order evolution equation. *IMA Journal of Numerical Analysis.* 2009;30(1):208–230.

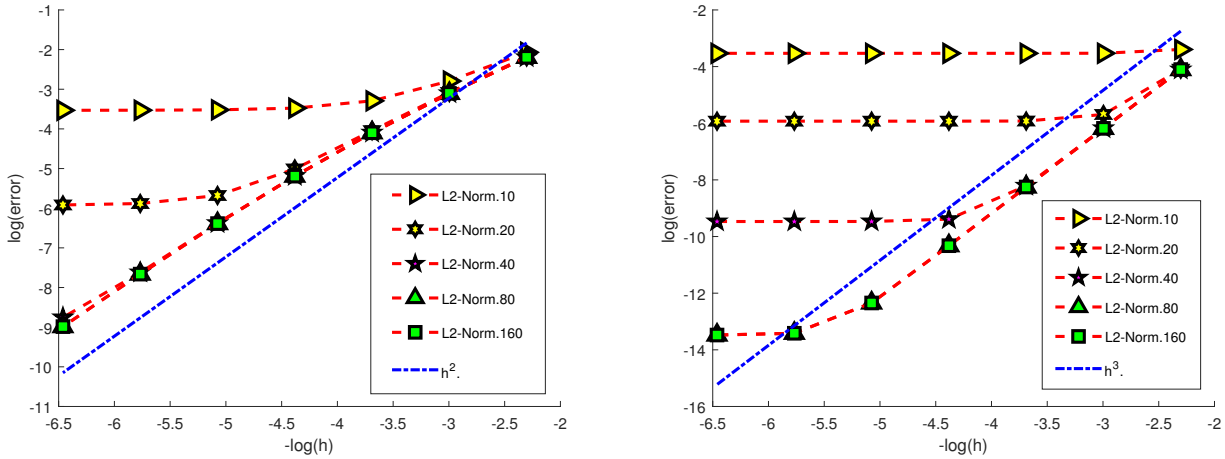


(a) degree of the polynomial, p=1 (b) degree of the polynomial, p=2

**FIGURE 5** Order of accuracy for Example 1 via $N_{Lap} = 10, 20, 40, 80, 160$.

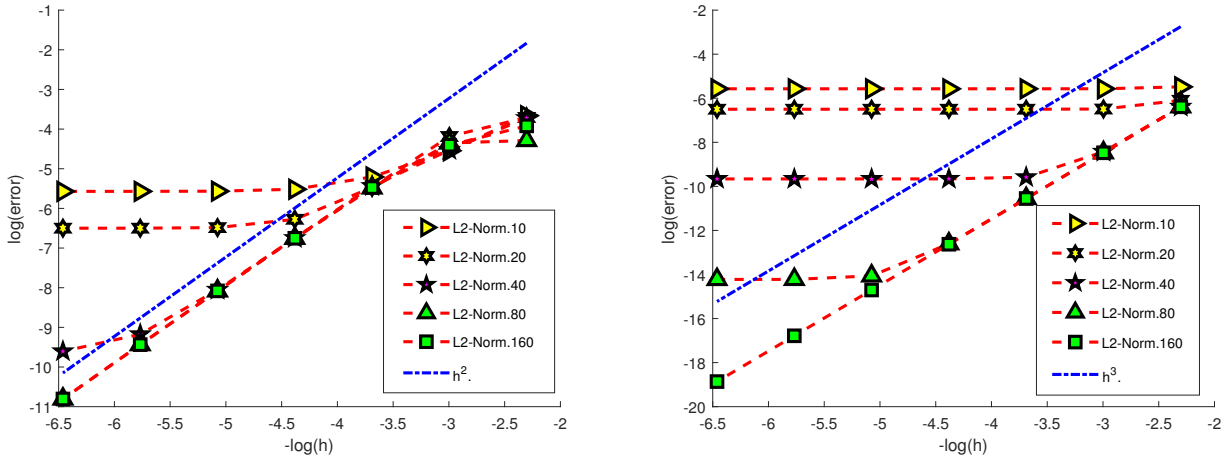


(a) degree of the polynomial, p=1 (b) degree of the polynomial, p=2

**FIGURE 6** Order of accuracy for Example 3 via $N_{Lap} = 10, 20, 40, 80, 160$.

16. McLean W, Thomée V. Numerical solution via Laplace transforms of a fractional order evolution equation. *The Journal of Integral Equations and Applications.* 2010;22(1):57–94.

17. Le Gia Q T, McLean W. Numerical solution of a parabolic equation on the sphere using Laplace transforms and radial basis functions. *ANZIAM Journal.* 2010;52:89–102.

18. Le Gia Q T, McLean W. Solving the heat equation on the unit sphere via Laplace transforms and radial basis functions. *Advances in Computational Mathematics.* 2014;40(2):353–375.

19. Gorenflo R, Luchko Y, Stojanović M. Fundamental solution of a distributed order time-fractional diffusion-wave equation as probability density. *Fractional Calculus and Applied Analysis.* 2013;16(2):297–316.

20. Jiao Z, Chen Y Q, Podlubny I. *Distributed-order dynamic systems: Stability, Simulation, Applications and Perspectives*. Springer-Verlag London; 2012.

21. Ye H, Liu F, Anh V. Compact difference scheme for distributed-order time-fractional diffusion-wave equation on bounded domains. *Journal of Computational Physics.* 2015;298:652–660.

22. Li X, Rui H. A block-centered finite difference method for the distributed-order time-fractional diffusion-wave equation. *Applied Numerical Mathematics.* 2018;131(1):123–139.

23. Li X, Rui H. A block-centred finite difference method for the distributed-order differential equation with Neumann boundary condition. *International Journal of Computer Mathematics.* 2019;96(3):622–639.

24. Ran M, Zhang C. New compact difference scheme for solving the fourth-order time fractional sub-diffusion equation of the distributed order. *Applied Numerical Mathematics.* 2018;129:58–70.

25. Chen H, Lü S, Chen W. Finite difference/spectral approximations for the distributed order time fractional reaction–diffusion equation on an unbounded domain. *Journal of Computational Physics.* 2016;315:84–97.

26. Guo S, Mei L, Zhang Z, Jiang Y. Finite difference/spectral-Galerkin method for a two-dimensional distributed-order time–space fractional reaction–diffusion equation. *Applied Mathematics Letters.* 2018;85:157–163.

27. Ren J, Chen H. A numerical method for distributed order time fractional diffusion equation with weakly singular solutions. *Applied Mathematics Letters.* 2019;96:159–165.

28. Wei L. A fully discrete LDG method for the distributed-order time-fractional reaction–diffusion equation. *Bulletin of the Malaysian Mathematical Sciences Society.* 2019;42(3):979–994.

29. Abbaszadeh M, Dehghan M. An improved meshless method for solving two-dimensional distributed order time-fractional diffusion-wave equation with error estimate. *Numerical Algorithms.* 2017;75(1):173–211.

30. Abbaszadeh M, Dehghan M. Meshless upwind local radial basis function-finite difference technique to simulate the time-fractional distributed-order advection–diffusion equation. *Engineering with Computers.* 2019;:1–17.

31. Liu Q, Mu S, Liu Q, et al. An RBF based meshless method for the distributed order time fractional advection–diffusion equation. *Engineering Analysis with Boundary Elements.* 2018;96:55–63.

32. Gao G H, Sun H-W, Sun Z-Z. Some high-order difference schemes for the distributed-order differential equations. *Journal of Computational Physics.* 2015;298:337–359.

33. Jin B, Lazarov R, Sheen D, Zhou Z. Error estimates for approximations of distributed order time fractional diffusion with nonsmooth data. *Fractional Calculus and Applied Analysis.* 2016;19(1):69–93.

34. Podlubny I. *Fractional differential equations: an introduction to fractional derivatives, fractional differential equations, to methods of their solution and some of their applications*. Vol. 198, Elsevier; 1998.

35. Hesthaven J S, Warburton T. *Nodal discontinuous Galerkin methods: Algorithms, Analysis, and Applications*. Springer-Verlag New York; 2007.